Journal of Mathematical Sciences, Vol. 193, No. 3, September, 2013

ALGEBRAIC ASPECTS OF THE HOFSTADTER PROBLEM IN GRAPHENE

M. Eliashvili and G. Tsitsishvili UDC 512.5

Abstract. We consider the Hofstadter problem on a honeycomb lattice. ita relevance to the quantum group $U_q(sl_2)$ is explicitly shown. We point out the reducibility of the corresponding characteristic polynomials and conjecture its relation to supersymmetric quantum mechanics.

1. Introduction

The problem of electrons moving in a periodic potential under the influence of an external magnetic field has been investigated since the beginning of quantum mechanics. Electronic systems confined to two spatial dimensions and subject to magnetic field comprise such utmost mathematical constructions as noncommutative geometry and quantum groups. This was the main source of the special interest in the corresponding studies. This interest has significantly grown due to the appearance of real two-dimensional electronic systems where the quantum Hall effect was discovered in the early 1980's. Later on, a new material, named graphene, was manufactured and led to further motivation for the aforementioned studies. Nowadays, quantum Hall physics and graphene physics represent natural arenas where modern mathematical ideas can be examined in reality. In what follows we discuss some facts traced out in graphene systems that apparently exhibit algebraic origins.

This paper is organized as follows. In Sec. 2, we briefly describe the tight-binding model of graphene. In Sec. 3, we describe the ab initio inclusion of the magnetic field in the tight-binding Hamiltonian. In Sec. 4, we show the relation to the quantum group $U_q(sl_2)$. In Sec. 5, we comment on the properties of characteristic polynomials, and in Sec. 6, we discuss its connection to supersymmetric quantum mechanics.

2. Tight-Binding Model

Graphene represents a one-atom-thick layer where the carbon atoms are organized in a honeycomb lattice, as depicted in Fig. 1.

The honeycomb lattice does not form the Bravais lattice but consists of two triangular Bravais sublattices. In this connection the lattice points are classified into two groups, indicated in Fig. 1 as empty and black circles. They can be parameterized as

$$\boldsymbol{r}_{\circ j_1 j_2} = \boldsymbol{R}_{j_1 j_2} - \frac{1}{2}\boldsymbol{\delta}_3, \tag{1a}$$

$$\boldsymbol{r}_{\bullet j_1 j_2} = \boldsymbol{R}_{j_1 j_2} + \frac{1}{2}\boldsymbol{\delta}_3, \tag{1b}$$

$$\boldsymbol{R}_{j_1 j_2} = j_1 \boldsymbol{a}_1 + j_2 \boldsymbol{a}_2, \tag{1c}$$

where the shift by $\frac{1}{2}\boldsymbol{\delta}_3$ specifies the reference frame.

Translated from Sovremennaya Matematika i Ee Prilozheniya (Contemporary Mathematics and Its Applications), Vol. 80, Proceedings of the International Conference "Modern Algebra and Its Applications" (Batumi, 2011), Part 1, 2012.

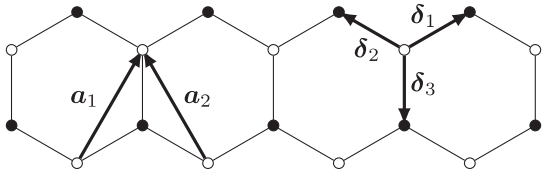

Fig. 1. The vectors $\boldsymbol{a}_1 = \frac{1}{2}(+1, \sqrt{3})$ and $\boldsymbol{a}_2 = \frac{1}{2}(-1, \sqrt{3})$ set the triangular Bravais lattice.

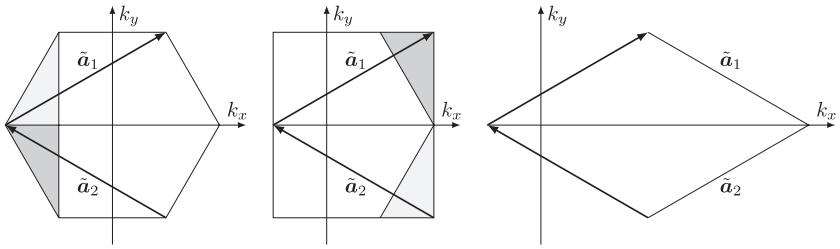

Fig. 2

One of the constructions adequately describing graphene is the so-called tight-binding model where the electrons can hop back and forth among the nearest neighboring sites. The corresponding Hamiltonian takes the form

$$H = \sum_{j_1 j_2} \Big[C^{\dagger}_{\bullet j_1+1, j_2} C_{\circ j_1 j_2} + C^{\dagger}_{\bullet j_1, j_2+1} C_{\circ j_1 j_2} + C^{\dagger}_{\bullet j_1 j_2} C_{\circ j_1 j_2} \Big] + h.c., \tag{2}$$

where $C^{\dagger}_{\mu j_1 j_2}$ are the electron creation operators ($\mu = \circ, \bullet$) and $C_{\mu j_1 j_2}$ are the annihilation ones. They satisfy the anticommutation relations

$$\big\{ C_{\mu i_1 i_2},\ C^{\dagger}_{\nu j_1 j_2} \big\} = \delta_{\mu\nu} \delta_{i_1 j_2} \delta_{i_2 j_2}. \tag{3}$$

The indicated terms of (2) describe the hopping of an electron from the white site at $\boldsymbol{r}_{\circ j_1 j_2}$ to the three nearest neighboring black sites, while the hermitian conjugate piece corresponds to the inverse processes.

The standard problem arising in physical studies is to investigate the spectrum of quadratic Hamiltonians, i.e., to diagonalize the corresponding quadratic forms. As usual, such a task is much easier to carry out in Fourier representation.

For the white and black sublattices, we have the Fourier representations

$$C_{\mu j_1 j_2} = \frac{1}{\sqrt{\Omega_{\mathrm{BZ}}}} \int\limits_{\mathrm{BZ}} e^{+i \boldsymbol{k} \boldsymbol{R}_{j_1 j_2}} c_{\mu}(\boldsymbol{k}) d\boldsymbol{k}, \tag{4}$$

where the integrations cover the Brillouin zone shown in the left panel of Fig. 2.

The operators $c_{\mu}(\boldsymbol{k})$ are invariant under the shifts $\boldsymbol{k} \to \boldsymbol{k} + \widetilde{\boldsymbol{a}}_{1,2}$, where the vectors $\widetilde{\boldsymbol{a}}_{1,2}$ referred to as the dual to $\boldsymbol{a}_{1,2}$ are defined by

$$\boldsymbol{a}_i \widetilde{\boldsymbol{a}}_j = 2\pi \delta_{ij} \tag{5}$$

Using the invariance $c_{\mu}(\boldsymbol{k} + \widetilde{\boldsymbol{a}}_j) = c_{\mu}(\boldsymbol{k})$, we can can arrange the hexagonal Brillouin zone in different ways, as shown in Fig. 2. They are all equivalent and are usually chosen in accord with particular technical needs.

Substituting (4) into (2) and performing the standard steps of discrete Fourier analysis, we find

$$H = \int\limits_{\mathrm{BZ}} \begin{pmatrix} c_{\circ}(\boldsymbol{k}) \\ c_{\bullet}(\boldsymbol{k}) \end{pmatrix}^{\dagger} \begin{pmatrix} 0 & f(\boldsymbol{k}) \\ f^*(\boldsymbol{k}) & 0 \end{pmatrix} \begin{pmatrix} c_{\circ}(\boldsymbol{k}) \\ c_{\bullet}(\boldsymbol{k}) \end{pmatrix} d\boldsymbol{k}, \tag{6}$$

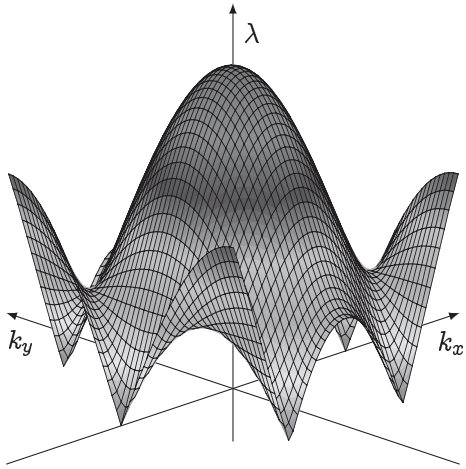

Fig. 3. The positive branch of the spectrum versus $\boldsymbol{k}$.

where $f(\boldsymbol{k}) = 1 + e^{+i\boldsymbol{k}\boldsymbol{a}_1} + e^{+i\boldsymbol{k}\boldsymbol{a}_2}$.

The term "spectrum" implies the eigenvalues of the matrix kernel standing in the integrand. In the case of (6), these eigenvalues are

$$\lambda = \pm|f(\boldsymbol{k})| = \sqrt{1 + 4\cos\left(\frac{1}{2}k_x\right)\cos\left(\frac{1}{2}\sqrt{3}k_y\right) + 4\cos^2\left(\frac{1}{2}k_x\right)} \tag{7}$$

and specify how the energy λ depends on the momentum $\boldsymbol{k}$. In Fig. 3, we plot $\lambda > 0$ versus $\boldsymbol{k}$.

3. Tight-Binding Model in Magnetic Field

We now turn to the homogeneous magnetic field orthogonal to the plane $\boldsymbol{B} = (0, 0, -B)$. In the tight-binding Hamiltonian, this corresponds to the "Peierls substitution"

$$H = \sum_{j_1 j_2}\left[e^{-i\gamma_1}C^\dagger_{\bullet j_1+1, j_2}C_{\circ j_1 j_2} + e^{-i\gamma_2}C^\dagger_{\bullet j_1, j_2+1}C_{\circ j_1 j_2} + e^{-i\gamma_3}C^\dagger_{\bullet j_1 j_2}C_{\circ j_1 j_2}\right] + \text{h.c.}, \tag{8}$$

where

$$\gamma_s(j_1, j_2) = \int\limits_{\boldsymbol{R}_{j_1 j_2} - \frac{1}{2}\boldsymbol{\delta}_3}^{\boldsymbol{R}_{j_1 j_2} - \frac{1}{2}\boldsymbol{\delta}_3 + \boldsymbol{\delta}_s} \boldsymbol{A}d\boldsymbol{l} \tag{9}$$

and $\boldsymbol{A} = (By, 0)$ is the vector-potential corresponding to the magnetic field $\boldsymbol{B} = \operatorname{rot}\boldsymbol{A}$.

The important property of the system set by (8) and (9) is the gauge invariance. If $\phi(\boldsymbol{r})$ is a function, then the Hamiltonian (8) remains invariant under the following transformations:

$$\boldsymbol{A} \longrightarrow \boldsymbol{A} + \boldsymbol{\partial}\phi, \tag{10a}$$

$$C_{\circ j_1 j_2} \longrightarrow e^{-i\phi(\boldsymbol{R}_{j_1 j_2} - \frac{1}{2}\boldsymbol{\delta}_3)}C_{\circ j_1 j_2}, \tag{10b}$$

$$C_{\bullet j_1 j_2} \longrightarrow e^{-i\phi(\boldsymbol{R}_{j_1 j_2} + \frac{1}{2}\boldsymbol{\delta}_3)}C_{\bullet j_1 j_2}. \tag{10c}$$

Note that in (10a) the magnetic field is unaffected. The Peierls substituion is nothing else but the realization of the gauge invariance, which is one of the fundamental principles in physics.

Substituting (4) in (8), we obtain

$$H = \int\limits_{\text{BZ}}\left\{e^{-i\boldsymbol{k}\boldsymbol{a}_1}c^\dagger_\bullet(\boldsymbol{k})c_\circ(\boldsymbol{k} + \boldsymbol{k}_\text{m}) + e^{-i(\boldsymbol{k} - \boldsymbol{k}_\text{m})\boldsymbol{a}_2}c^\dagger_\bullet(\boldsymbol{k})c_\circ(\boldsymbol{k} - \boldsymbol{k}_\text{m}) + c^\dagger_\bullet(\boldsymbol{k})c_\circ(\boldsymbol{k})\right\}d\boldsymbol{k} + \text{h.c.}, \tag{11}$$

where $\boldsymbol{k}_{\mathfrak{m}} = (0, B/2)$.

Compared with (6) the quadratic form (11) is complicated since the infinite amount of $\boldsymbol{k}$'s are entangled among each other. Relative simplification is achieved by considering the special values of the magnetic field set by

$$B = \frac{4\pi}{\sqrt{3}\,a}\,\frac{\nu}{N},$$

where N and ν are positive coprime integers. Then the magnetic flux per the elementary hexagon ($B\times$area) is rational (ν/N) of 2π, and the infinite-dimensional system decouples into finite-dimensional blocks, where the diagonalization can be carried out independently. In this case, we have

$$\boldsymbol{k}_{\mathfrak{m}} = \frac{2\pi}{\sqrt{3}\,a}\,\frac{\nu}{N}\,(0,1)$$

and (11) can be rewritten as follows:

$$H = \int\limits_{\mathrm{RBZ}} \Psi^{\dagger}(\boldsymbol{k})\mathcal{H}(\boldsymbol{k})\Psi(\boldsymbol{k})d\boldsymbol{k}, \tag{12}$$

where

$$\Psi(\boldsymbol{k}) = \big\{\Psi_{\circ}(\boldsymbol{k}),\ \Psi_{\bullet}(\boldsymbol{k})\big\}, \quad \Psi_{\mu}(\boldsymbol{k}) = \big\{c_{\mu}(\boldsymbol{k}),\ c_{\mu}(\boldsymbol{k}-\boldsymbol{k}_{\mathfrak{m}}),\ \ldots,\ c_{\mu}(\boldsymbol{k}-N\boldsymbol{k}_{\mathfrak{m}}+\boldsymbol{k}_{\mathfrak{m}})\big\},$$

and the integration is extended over the reduced Brillouin zone (RBZ), implying its area is N times less than that of the Brillouin zone.

The kernel $\mathcal{H}(\boldsymbol{k})$, which is the main object of interest, has the form

$$\mathcal{H} = \begin{pmatrix} 0 & \Delta^{\dagger} \\ \Delta & 0 \end{pmatrix}, \tag{13}$$

where

$$\Delta = \mathbb{I} + e^{-i\boldsymbol{k}\boldsymbol{a}_1}\beta^{\dagger}\Pi + e^{-i\boldsymbol{k}\boldsymbol{a}_2}\Pi\beta, \tag{14a}$$

$$\beta = \begin{pmatrix} 0 & 1 & 0 & \cdots & 0 & 0 \\ 0 & 0 & 1 & \cdots & 0 & 0 \\ 0 & 0 & 0 & \cdots & 0 & 0 \\ \vdots & \vdots & \vdots & \ddots & \vdots & \vdots \\ 0 & 0 & 0 & \cdots & 0 & 1 \\ 1 & 0 & 0 & \cdots & 0 & 0 \end{pmatrix}, \tag{14b}$$

$$\Pi = \mathrm{diag}\left(q^1, q^2, \ldots, q^N\right), \tag{14c}$$

$$q = e^{+i\pi(\nu/N)}, \tag{14d}$$

and $\mathbb{I}$ is the identity matrix.

The subject of our studies is the eigenvalue spectrum of operator (13). The related eigenvalue equation is

$$\Delta\xi = \lambda\zeta, \tag{15a}$$

$$\Delta^{\dagger}\zeta = \lambda\xi, \tag{15b}$$

where ξ and ζ are N-component columns. If (λ, ξ, ζ) is a solution of (15), then $(-\lambda, \xi, -\zeta)$ is also a solution, i.e., each positive eigenvalue possesses a negative partner. Therefore, it suffices to search for the eigenvalues λ^2. These appear after squaring up (15):

$$\Delta^{\dagger}\Delta\xi = \lambda^2\xi, \tag{16a}$$

$$\Delta\Delta^{\dagger}\zeta = \lambda^2\zeta, \tag{16b}$$

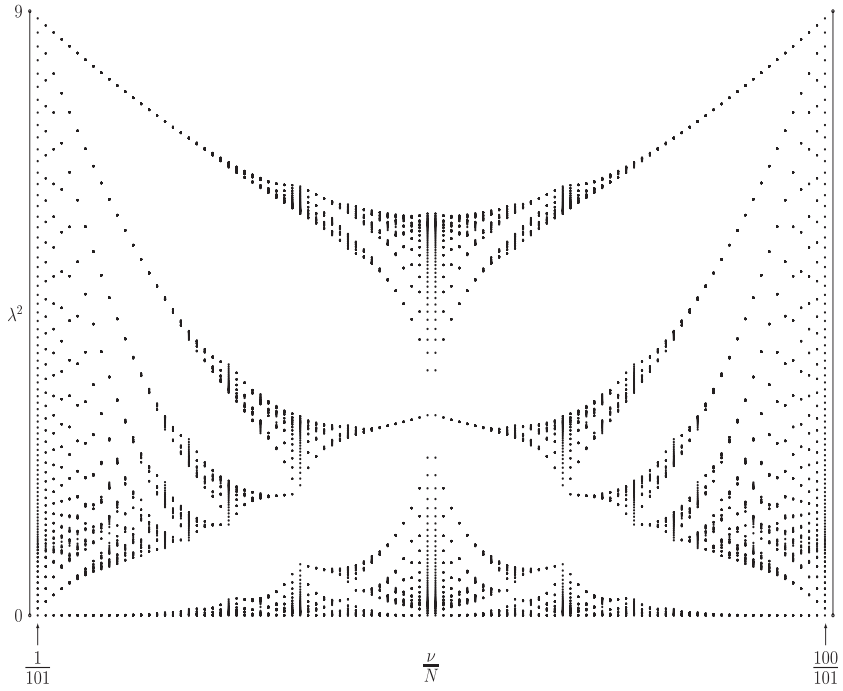

Fig. 4. Eigenvalues λ^2 versus the ratio $\frac{\nu}{N}$, $\nu = 1, 2, \ldots, 100$, $N = 101$. The energy eigenvalues are bounded as $\lambda^2 \leq 9$.

where ξ and ζ are now decoupled. Each of these equations has N eigenpairs (λ_n^2, ξ_n) and (λ_n^2, ζ_n) with $n = 1, 2, \ldots, N$.

The basic motivation for such considerations has its origin in the work of Hofstadter [4] where the similar eigenvalue problem was considered on a square lattice and the so-called Hofstadter butterfly was introduced. The subsequent extensive studies showed that the eigenvalue spectrum of a tight-binding model on a square lattice exhibits the fractal structure. Similar considerations have been carried out also for the honeycomb lattice, which, however, are based mostly on numeric calculations. In Fig. 4, the Hofstadter butterfly for the honeycomb lattice is shown.

The Hofstadter butterfly exposes how the eigenvalues λ_n depend on the value of the applied magnetic field (the value of ν/N). In order to make things clearer we comment on how the diagram is constructed. We take $N = 101$ (higher N's require higher computer resources) and $\nu = 1$. In this case, we have 101 eigenvalues set by (16). We compute these eigenvalues numerically and plot them in increasing order along the first vertical in the figure. We then perform the same operations for $\nu = 2$. We obtain 101 eigenvalues, which, however, differ from those for $\nu = 1$. We plot them along the second vertical, and so on up to $\nu = 100$ (later on we argue that the dependence of the eigenvalues on $\boldsymbol{k}$ disappears when N is sufficiently large, and therefore the particular value of $\boldsymbol{k}$ is not important and is usually fixed for convenience in numerical calculations).

Undoubtedly, the structure of the diagram is highly nontrivial. The existence of certain regions where the eigenvalues are located is evident. Such regions are separated one from another by gaps. In mathematics these can be well described by applying the discrete Hill's equation (see, e.g., [7]). The discrete Hill's equation admits two kinds of solutions—stable and unstable. The stable ones are in fact the normalizable (finite norm) states, which carry the physical sense, and the corresponding eigenvalues are those indicated in the Hofstadter diagram. The unstable solutions imply the divergent norm. The corresponding eigenvalues appear inside the gaps and are not indicated since they are physically irrelevant.

As we have already mentioned, the Hofstadter problem for a honeycomb lattice has been widely studied, but the methods employed are exceptionally numerical. In our studies we basically aim to develop an analytic approach to the problem. At the current stage, the results are fragmental, but nevertheless the observations are quite interesting. In what follows we comment on its relation to quantum groups, and also on the reducibility of characteristic polynomials.

4. Quantum Algebra $U_q(sl_2)$

Introduce

$$X^+ = \frac{e^{-i\boldsymbol{k}\boldsymbol{a}_1}\beta^\dagger\Pi + e^{-i\boldsymbol{k}\boldsymbol{a}_2}\Pi\beta}{i(q-q^{-1})}, \tag{17a}$$

$$X^- = \frac{e^{+i\boldsymbol{k}\boldsymbol{a}_1}\Pi^\dagger\beta + e^{+i\boldsymbol{k}\boldsymbol{a}_2}\beta^\dagger\Pi^\dagger}{i(q-q^{-1})}. \tag{17b}$$

Then operator (13) has the form

$$\mathcal{H} = \begin{pmatrix} 0 & \mathbf{1} + i(q-q^{-1})X^- \\ \mathbf{1} + i(q-q^{-1})X^+ & 0 \end{pmatrix}. \tag{18}$$

Using the relation

$$\Pi^\dagger\beta\Pi = q^2\Pi\beta\Pi^\dagger,$$

which in fact represents the Heisenberg–Weyl algebra, we obtain

$$[X^+, X^-] = \frac{K - K^{-1}}{q - q^{-1}}, \tag{19}$$

where

$$K = qe^{+i\boldsymbol{k}(\boldsymbol{a}_1-\boldsymbol{a}_2)}\Pi\beta\Pi^\dagger\beta, \tag{20a}$$

$$K^{-1} = q^{-1}e^{-i\boldsymbol{k}(\boldsymbol{a}_1-\boldsymbol{a}_2)}\beta^\dagger\Pi\beta^\dagger\Pi^\dagger. \tag{20b}$$

The rest of the commutation relations can be summarized in

$$KX^\pm K^{-1} = q^{\pm 2}X^\pm, \tag{21}$$

i.e., the operators $X^\pm$, K, and K^{-1} form the algebra $U_q(sl_2)$.

5. Secular Equation and Reducibility

Explicit calculations are easier in the basis where K and K^{-1} are diagonal. For $\nu = even$, this can be achieved involving the eigenvectors of the β given by (hereafter we continue with $\nu = even$)

$$h_\kappa^T = \frac{1}{\sqrt{N}}\{q^\kappa, q^{2\kappa}, q^{3\kappa}, \ldots, q^{N\kappa}\}. \tag{22}$$

These states satisfy the cyclic property

$$h_{\kappa+N} = h_\kappa,$$

which is employed in further manipulations and is valid due to $q^N = 1$, which in turn follows from $\nu = even$. Namely, states (22) satisfy the relations

$$h_\kappa^\dagger h_{\kappa'} = \delta_{\kappa\kappa'}, \tag{23a}$$

$$\beta h_\kappa = q^\kappa h_\kappa \quad\Longrightarrow\quad h_\kappa^\dagger\beta h_{\kappa'} = (\Pi)_{\kappa\kappa'}, \tag{23b}$$

$$\beta^\dagger h_\kappa = q^{-\kappa} h_\kappa \quad\Longrightarrow\quad h_\kappa^\dagger\beta^\dagger h_{\kappa'} = (\Pi^\dagger)_{\kappa\kappa'}, \tag{23c}$$

$$\Pi h_\kappa = h_{\kappa+1} \quad\Longrightarrow\quad h_\kappa^\dagger\Pi h_{\kappa'} = (\beta^\dagger)_{\kappa\kappa'}, \tag{23d}$$

$$\Pi^\dagger h_\kappa = h_{\kappa-1} \quad\Longrightarrow\quad h_\kappa^\dagger\Pi^\dagger h_{\kappa'} = \beta_{\kappa\kappa'}. \tag{23e}$$

Performing the transformation $\Delta \to \widetilde{\Delta} = W^\dagger \Delta W$ with the unitary matrix set by $W_{n\kappa} = (h_\kappa)_n$, we transform the operator $\mathcal{H}$ into

$$\mathcal{H} \to \widetilde{\mathcal{H}} = \begin{pmatrix} 0 & \widetilde{\Delta}^\dagger \\ \widetilde{\Delta} & 0 \end{pmatrix}, \tag{24}$$

where

$$\widetilde{\Delta} = \mathbb{I} + e^{-i\boldsymbol{k}\boldsymbol{a}_1}\Pi^\dagger\beta^\dagger + e^{-i\boldsymbol{k}\boldsymbol{a}_2}\beta^\dagger\Pi. \tag{25}$$

Substituting the explicit values of $a_{1,2}$ and that of q we find

$$\widetilde{\Delta} = \mathbb{I} + e^{-\frac{i}{2}\sqrt{3}k_y - \frac{i\pi\nu}{2N}}\, T, \tag{26a}$$

$$T = \begin{pmatrix} 0 & 0 & 0 & \dots & 0 & t_1 \\ t_2 & 0 & 0 & \dots & 0 & 0 \\ 0 & t_3 & 0 & \dots & 0 & 0 \\ \vdots & \vdots & \vdots & \ddots & \vdots & \vdots \\ 0 & 0 & 0 & \ddots & 0 & 0 \\ 0 & 0 & 0 & \ddots & t_N & 0 \end{pmatrix}, \tag{26b}$$

$$t_n = 2\cos\left(\pi\frac{\nu}{N}n + \frac{1}{2}k_x - \frac{\pi\nu}{2N}\right). \tag{26c}$$

The eigenvalue spectra of $\mathcal{H}$ and $\widetilde{\mathcal{H}}$ are identical, but $\widetilde{\mathcal{H}}$ is easier to deal with, since the structure of $\widetilde{\Delta}$ is simpler than the one of Δ. Instead of (16) we now have the equations

$$\widetilde{\Delta}^\dagger\widetilde{\Delta}\xi = \lambda^2\xi, \tag{27a}$$

$$\widetilde{\Delta}\widetilde{\Delta}^\dagger\zeta = \lambda^2\zeta. \tag{27b}$$

The secular equation determining the eigenvalues λ_n^2 has the form $\Omega_N^\nu(\lambda^2) = 0$, where the characteristic polynomial is defined by

$$\Omega_N^\nu(\lambda^2) = \det\left|\widetilde{\Delta}^\dagger\widetilde{\Delta} - \mathbb{I}\cdot\lambda^2\right| = \det\left|\widetilde{\Delta}\widetilde{\Delta}^\dagger - \mathbb{I}\cdot\lambda^2\right|. \tag{28}$$

Below we point out some properties of $\Omega_N^\nu(\lambda^2)$ that are obtained empirically. For this purpose let us present $\Omega_N^\nu(\lambda^2)$ in the form of the power expansion

$$\Omega_N^\nu(\lambda^2) = \omega_N\lambda^{2N} + \omega_{N-1}\lambda^{2(N-1)} + \dots + \omega_2\lambda^4 + \omega_1\lambda^2 + \omega_0. \tag{29}$$

The coefficients ω_n must depend on $\boldsymbol{k}$, since the matrix elements of $\widetilde{\Delta}(\boldsymbol{k})$ do. However, we find that only ω_0 depends on $\boldsymbol{k}$ while the rest are all $\boldsymbol{k}$-independent. This observation resembles the case of a square lattice where the same property originates from the gauge invariance (see [8]). In our case the gauge invariance is described by (10).

Since $\omega_{n\neq 0}$ is the only $\boldsymbol{k}$-independent piece of $\Omega_N^\nu(\lambda^2)$, it is reasonable to separate out this term explicitly. Then the secular equation is

$$\Omega_N^\nu(0) - \Omega_N^\nu(\lambda^2) = 1 + 4\cos\left(\frac{1}{2}Nk_x\right)\cos\left(\frac{\sqrt{3}}{2}Nk_y\right) + 4\cos^2\left(\frac{1}{2}Nk_x\right), \tag{30}$$

where we have used the explicit analytic expression of ω_0. Note that the right-hand side of (30) has the same form as in (7).

As an examples we present some particular expressions

$$\Omega_3^\nu(0) - \Omega_3^\nu(x) = 18x - 9x^2 + x^3, \tag{31a}$$

$$\Omega_5^\nu(0) - \Omega_5^\nu(x) = (90 + 15w)x - (145 + 5w)x^2 + 75x^3 - 15x^4 + x^5, \tag{31b}$$

$$\begin{aligned}\Omega_7^\nu(0) - \Omega_7^\nu(x) = {} & (217 + 126w + 56w^2)x - (1008 + 168w + 21w^2)x^2 \\ & + (1218 + 63w)x^3 - (644 + 7w)x^4 + 168x^5 - 21x^6 + x^7,\end{aligned} \tag{31c}$$

$$\begin{aligned}\Omega_9^\nu(0) - \Omega_9^\nu(x) = {} & (135 + 621w + 405w^2)x - (4239 + 1728w + 567w^2)x^2 \\ & + (10314 + 1719w + 225w^2)x^3 \\ & - (10503 + 729w + 27w^2)x^4 + (5643 + 135w)x^5 \\ & - (1719 + 9w)x^6 + 297x^7 - 27x^8 + x^9,\end{aligned} \tag{31d}$$

where $w = 2\cos(2\pi\nu/N)$.

Now we comment on the reducibility properties of $\Omega_N^\nu(0) - \Omega_N^\nu(x)$ observed for some low values of N. The cases of $N = 3$ and $N = 5$ are trivial since the polynomials are effectively quadratic and quartic due to the absence of the lowest power. We comment on $N = 7$ and $N = 9$. Let us first remark that the quantity w is related to the division of a circle into N equal sectors and therefore satisfies certain relations which for $N = 7$ looks like $w^3 + w^2 - 2w - 1 = 0$, while for $N = 9$ it takes the form $w^3 - 3w + 1 = 0$. The involved polynomials are referred to as the minimal polynomials.

Provided w is the root of the minimal polynomial, we find the following relations:

$$\Omega_7^\nu(0) - \Omega_7^\nu(x) = xP_2(x)Q_4(x), \tag{32}$$

where

$$P_2(x) = x^2 - (3 + w^2)x + (1 + w + w^2), \tag{33a}$$

$$\begin{aligned}Q_4(x) = {} & x^4 - (18 - w^2)x^3 + (112 - 2w - 13w^2)x^2 \\ & - (279 - 13w - 51w^2)x + (233 - 16w - 59w^2),\end{aligned} \tag{33b}$$

and

$$\Omega_9^\nu(0) - \Omega_9^\nu(x) = x(x - 4 + w^2)(x - 2 - w^2)P_3(x)Q_3(x), \tag{34}$$

where

$$P_3(x) = x^3 - 9x^2 + (14 + w + 2w^2)x - 3w - 3w^2, \tag{35a}$$

$$Q_3(x) = x^3 - 12x^2 + (41 - 2w - w^2)x - 36 + 3w + 3w^2. \tag{35b}$$

Polynomials are usually regarded as defined over the field containing their coefficients. In our case, this is the field of rational numbers (or maybe the ring of integers) extended by an element w. Obviously the constituent polynomials (P and Q) are defined over the same field as the original ones. This is an indication of the reducibility, which must have a certain algebraic origin.

In Fig. 5, we plot $\lambda^2(\boldsymbol{k})$ versus $\boldsymbol{k}$ for $\nu/N = 2/3$. According to (31) and (32), these are set by

$$\lambda^6 - 9\lambda^4 + 18\lambda^2 = 1 + 4\cos\left(\frac{3}{2}\,k_x\right)\cos\left(\frac{3}{2}\sqrt{3}\,k_y\right) + 4\cos^2\left(\frac{3}{2}k_x\right) \tag{36}$$

and give out three surfaces of $\lambda^2(\boldsymbol{k})$. Increasing N, we will observe N such surfaces. We empirically conclude that these surfaces have no touch points. Employing the Gerschgorin circles [5], we find that the eigenvalues are bounded as $|\lambda| \le 3$ (the number 3 originates from the fact that every site has three neighboring ones where the electron can hop to). Hence the values of λ^2 are bounded from above by $\lambda^2 \le 9$. Therefore, increasing N, the surfaces become multiplied without touching each other, which means that they become flat, i.e., the dependence on $\boldsymbol{k}$ disappears. Therefore, provided that N is large, the value of $\boldsymbol{k}$ can be chosen to meet any auxiliary requirement.

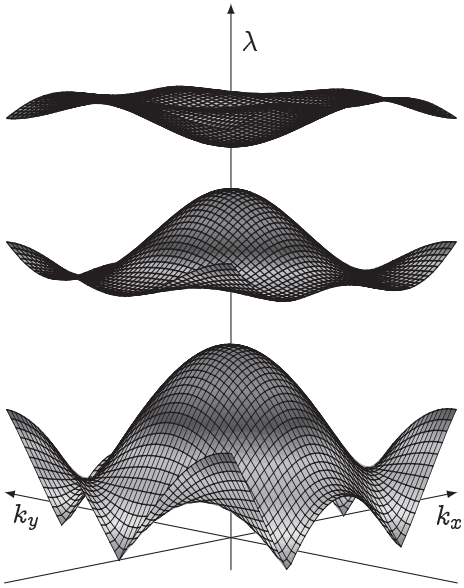

Fig. 5. Positive branches of the case $\nu/N = 2/3$. The reduced Brillouin zone is 1/3 of the original Brillouin zone. Conversely, the amount of bands (surfaces) is multiplied by 3.

6. Supersymmetry

Systems of equations like (27) are typical in the so-called supersymmetric quantum mechanics (see, e.g., [1]). The two operators $\mathcal{H}_+ = \widetilde{\Delta}^\dagger\widetilde{\Delta}$ and $\widetilde{\Delta}\widetilde{\Delta}^\dagger$ are referred to as the partner Hamiltonians. Apparently the spectra of $\mathcal{H}_\pm$ are positively defined and hence bounded from below. It is said that supersymmetry is unbroken if the lowest eigenvalue is exactly zero, otherwise the supersymmetry is broken. We relate this feature to the reducibility properties of characteristic polynomials described in Sec. 5. For the special values of $\boldsymbol{k}$ (e.g., $3Nk_x = 2\pi$ and $\sqrt{3}\,Nk_y = 2\pi$), the right-hand side of (30) vanishes, so the secular equation has the form

$$\Omega_N^\nu(0) - \Omega_N^\nu(\lambda^2) = 0 \tag{37}$$

and means that zero eigenvalues exist. They are given by

$$\begin{pmatrix} 0 & \widetilde{\Delta} \\ \widetilde{\Delta}^\dagger & 0 \end{pmatrix} \begin{pmatrix} 0 \\ \xi_0 \end{pmatrix} = \begin{pmatrix} 0 & \widetilde{\Delta} \\ \widetilde{\Delta}^\dagger & 0 \end{pmatrix} \begin{pmatrix} \zeta_0 \\ 0 \end{pmatrix} = 0, \tag{38}$$

where ξ_0 and ζ_0 are defined by

$$\widetilde{\Delta}\xi_0 = \widetilde{\Delta}^\dagger\zeta_0 = 0$$

and are easily soluble employing the explicit expression of $\widetilde{\Delta}$ set by (26a) and (26b).

Due to the reducibility of $\Omega_N^\nu(0) - \Omega_N^\nu(\lambda^2)$, the rest of the eigenvalues are expressible in radicals. In this respect, we conjecture that the unbroken supersymmetry must be equivalent to the solubility of the corresponding Galois groups.

REFERENCES

1. F. Cooper, A. Khare, and U. Sukhatme, *Phys. Rep.*, **251**, 267 (1995).
2. Z. F. Ezawa, *Quantum Hall Effects*, World Scientific (2008).
3. Y. Hasegawa et al., *Phys. Rev. Lett.*, **63**, 907 (1989).
4. D. R. Hofstadter, *Phys. Rev. B*, **14**, 2239 (1976).
5. C. D. Meyer, *Matrix Analysis and Applied Linear Algebra*, SIAM (2000).

6. G. W. Semenoff, *Phys. Rev. Lett.*, **53**, 2449 (1984).
7. M. Toda, *Theory of Nonlinear Lattices*, Springer-Verlag (1981).
8. P. B. Wiegmann and A. V. Zabrodin, *Phys. Rev. Lett.*, **72**, 1890 (1994).

M. Eliashvili
A. Razmadze Mathematical Institute, Tbilisi, Georgia
E-mail: simi@rmi.acnet.ge
G. Tsitsishvili
A. Razmadze Mathematical Institute, Tbilisi, Georgia
E-mail: gts@rmi.ge